SEARCH FOR CHARMLESS B-DECAYS

J. Fast
Physics Department, Purdue University,
West Lafayette, Indiana USA 47907

(Representing the CLEO collaboration)

We have searched for several two-body charmless hadronic decays of B mesons. These final states include $K\pi$ and $\pi\pi$ with both charged and neutral kaons and pions; $K^*\pi$, $K\rho$, and $\pi\rho$; and ϕX_s, where $X_s = K,\ K^*$, or ϕ. We have also searched for the decay $B \to \tau\bar{\nu}_\tau$. Using a dataset which includes 2.2 million $B\overline{B}$ pairs, we place upper limits on the charmless hadronic decay branching ratios in the range from 10^{-4} to 10^{-5}, and set a limit $BR(B \to \tau\bar{\nu}_\tau) < 2.2 \times 10^{-3}$.

1. Introduction

The decays of B-mesons to two charmless hadrons can proceed via a $b \to u$ tree-level spectator diagram (Fig. 1a), or via a $b \to sg$ one-loop "penguin-diagram" (Fig. 1b) and to a lesser extent, via the CKM-suppressed $b \to dg$ penguin diagram. Although rare decays can also proceed via $b \to u$ internal, color-suppressed diagrams (Fig. 1c), $b \to u$ exchange diagrams (Fig. 1d), annihilation diagrams (Fig. 1e), or vertical W loop diagrams (Fig. 1f), these contributions are expected to be negligible in most cases.

This paper reports preliminary results on the decays $B \to K\pi$, $B \to K^*\pi$, $B \to K\rho$, $B \to \pi\rho$, and $B \to X_s\phi$. We place upper limits on these modes in the range 10^{-4} to 10^{-5}.

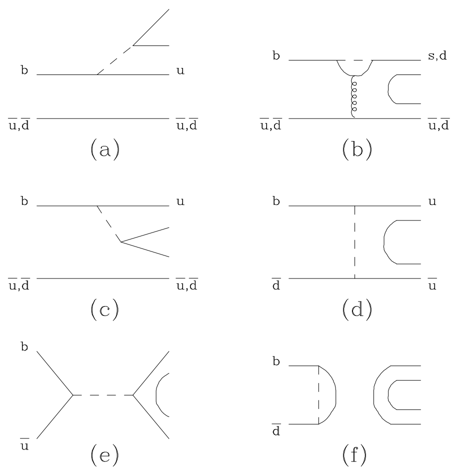

Fig. 1. Feynman diagrams: (a) external W emission, (b) loop or gluonic penguin, (c) internal W, (d) W exchange, (e) annihilation, and (f) vertical W loop.

We also include updated results on the decays $B^0 \to K^+\pi^-$, $B^0 \to \pi^+\pi^-$, and $B^0 \to K^+K^-$. A search is made for the decay $B \to \tau\bar{\nu}_\tau$ which proceeds through an annihilation diagram similar to that shown in Fig. 1e, and hence provides a measurement of $f_B|V_{ub}|$. This decay also probes physics beyond the standard model, such as annihilation to a charged Higgs. We set a limit of $BR(B \to \tau\bar{\nu}_\tau) < 2.2 \times 10^{-3}$ at the 90% confidence level.

2. Data sample

The data set used in this analysis was collected with the CLEO-II detector[1] at the Cornell Electron Storage Ring (CESR). It consists of 2.0 fb^{-1} taken on the $\Upsilon(4S)$ (on-resonance) and 1.0 fb^{-1} taken at a center of mass energy $\sim$ 55 MeV below the $\Upsilon(4S)$ (off-resonance). The on-resonance sample contains 2.2 million $B\overline{B}$ pairs. The off-resonance sample, taken below the $B\overline{B}$ threshold, is used for continuum background estimates.

3. Charmless Hadronic Decays

We provide here a brief overview of the analysis issues and tools used to address these concerns. A more detailed description of this analysis appears in.[2]

3.1. Background suppression

In general, $b \to c$ decays do not produce back-to-back particles with sufficient momentum to be a source of background to the rare decay modes under study; the dominant background comes from non-resonant (continuum) production of light quarks, $e^+e^- \to q\overline{q}$, $q = u, d, s, c$. Since B mesons from $\Upsilon(4S)$ decay are produced nearly at rest in the laboratory frame, the B decays are isotropic and the resulting event shape is rather spherical. Continuum background events naturally contain high momentum back-to-back particles in the two opposing light quark jets. We require $|\cos\theta_{thrust}| < 0.7$, where θ_{thrust} is the angle between the thrust axis of the candidate and that of the rest of the event. This cut removes $\sim$ 90% of the continuum background with $\sim$ 65% efficiency for signal events. Additional continuum suppression is achieved using a Fisher discriminant which reduces continuum backgrounds by a factor of 2 to 3, after requiring $|\cos\theta_{thrust}| < 0.7$, with efficiencies for signal events $\sim$ 80%.

In the process $e^+e^- \to \Upsilon(4S) \to B\overline{B}$, the B mesons are produced with the same energy as the colliding $e^\pm$ beams, E_{beam}. We define the variable $\Delta E = E_{candidate} - E_{beam}$. A signal region is defined by $|\Delta E| < 2.0 - 2.5\sigma$, where σ is the rms resolution determined from Monte Carlo studies. We also define the beam-constrained B mass as $M_B = \sqrt{E^2_{beam} - \vec{p}^{\,2}_{candidate}}$, where $\vec{p}_{candidate}$ is the vector sum of the momenta of the candidate daughters. The resolution in the beam-constrained mass, $\sigma = 2.6 \pm 0.2$ MeV, is dominated by the spread in beam energy. The signal region is defined as $|M_B - 5280| < 6 - 8$ MeV, depending on the decay mode under consideration.

3.2. Results

Results and a range of theoretical predictions for these decays appear in Table 1. The expected background in the signal region is obtained by scaling the number of events seen in a large sideband region in the ΔE *vs.* M_B plane.

Table 1. Event yields, estimated background in the signal region, upper limits on the branching ratios, previous upper limits, and theoretical predictions. Upper limits are at the 90% confidence level. For the decays $B \to X_s\phi$, particles in parentheses indicate a $K^*(892)$ decaying to those particles.

Mode	Event Yield	Est. Bkgr.	Upper Limit on BR (10^{-5})	Previous UL (10^{-5})	Theory (10^{-5})
$\pi^0\pi^0$	1	1.7 ± 0.4	1.0	–	0.03-0.10
$\pi^\pm\rho^\mp$	6	2.4 ± 0.6	9.5	52	1.9-8.8
$\pi^0\rho^0$	1	1.5 ± 0.5	2.9	40	0.07-0.23
$\pi^+\pi^0$	8	5.8 ± 0.6	2.3	24	0.6-2.1
$\pi^+\rho^0$	3	1.8 ± 0.3	4.1	15	0.0-1.4
$K^0\pi^0$	2		6.3	–	0.5-0.8
$K^{*+}\pi^-$	3	0.6 ± 0.2	23.8	44	0.1-1.9
$K^{*0}\pi^0$	0	0.9 ± 0.3	3.5	–	0.3-0.5
$K^+\rho^-$	2	1.7 ± 0.4	4.3	–	0.0-0.2
$K^0\phi$	1		10.7	49	0.1-1.3
$(K^+\pi^-)\phi$	1				
$(K^0\pi^0)\phi$	0				
$K^{*0}\phi$ (combined)	1		3.9	32	0.0-3.1
$\phi\phi$	0		4.8	–	–
$K^+\pi^0$	10	5.0 ± 0.5	3.2	–	0.3-1.3
$K^0\pi^+$	6	2.0 ± 0.5	6.8	9	1.1-1.2
$K^{*0}\pi^+$	2	0.6 ± 0.2	6.0	13	0.6-0.9
$K^+\rho^0$	1	1.1 ± 0.2	2.6	7	0.01-0.06
$K^+\phi$	0		1.4	8	0.1-1.5
$(K^+\pi^0)\phi$	0				
$(K^0\pi^+)\phi$	1				
$K^{*+}\phi$ (combined)	1		9.0	130	0.0-3.1

Our previously published results[3] for $B^0 \to K^+\pi^-$ and $B^0 \to \pi^+\pi^-$ showed a significant signal in the sum of the two modes. Since publication, we have added 50% more data. Updated results appear in Table 2. Our sensitivity is at the level of theoretical predictions for the modes $\pi^+\pi^-$, $K^+\pi^-$, $\pi^+\pi^0$, $\pi^\pm\rho^\mp$, $K^+\phi$, and $K^{*0}\phi$.

Table 2. Updated results for $B^0 \to K^+\pi^-$, $B^0 \to \pi^+\pi^-$, and $B^0 \to K^+K^-$. Upper limits are at the 90% confidence level.

Mode	Event Yield	BR (10^{-5})	Theoretical Predictions (10^{-5})[4]
$\pi^+\pi^-$	$8.5^{+4.9}_{-4.0}$	< 2.2	1.0-2.6
$K^+\pi^-$	$7.1^{+4.2}_{-3.4}$	< 1.9	1.0-2.0
K^+K^-	$0.0^{+1.6}_{-0.0}$	< 0.7	–
$\pi^+\pi^- + K^+\pi^-$	$15.7^{+5.3}_{-4.5}$	$1.8^{+0.6}_{-0.5} \pm 0.2$	

4. $B \to \tau\bar{\nu}_\tau$

This analysis is described in detail in.[5] We search for events in which the tau decays leptonically, and for which the other B-meson decay products are all hadronic. For these events the missing energy-momentum 4-vector for the event is equivalent, within detector resolution, to the 4-momentum of the three neutrinos. The single lepton is removed from the event, and then ΔE and M_B are calculated, as described above, using the remaining tracks and showers. This is equivalent to reconstructing the $B \to \tau\bar{\nu}_\tau$ decay. We subtract continuum background using scaled off-resonance data. A 2-dimensional fit is done in ΔE versus M_B for three components:(1)$B \to \tau\bar{\nu}_\tau$ signal, (2)$B\bar{B}$ background with primary leptons from semileptonic B decay, and (3)other $B\bar{B}$ backgrounds. The yield of $B \to \tau\bar{\nu}_\tau$ is found to be -14 ± 37 events, corresponding to an upper limit of $BR(B \to \tau\bar{\nu}_\tau) < 2.2 \times 10^{-3}$ at the 90% confidence level, two orders of magnitude above standard model predictions.

References

1. Y. Kubota *et al.* (CLEO), *Nucl. Instr. Methods A* **320** (1992) 66.
2. J. Gronberg *et al.* (CLEO), *ICHEP94 Ref. GSL0391* (1994).
3. M. Battle *et al.* (CLEO), *Phys. Rev. Lett.* **71** (1993) 3922.
4. A. Deandrea, N. Di Bartolomeo, R. Gatto, F. Feruglio, and G. Nardulli, *Phys. Lett. B* **320** (1994) 170; N. G. Deshpande and Xiao-Gang He, *OITS-538* (1994); A. Deandrea, N. Di Bartolomeo, R. Gatto, and G. Nardulli, *Phys. Lett. B* **318** (1993) 549; A.J. Davies, T. Hayashi, M. Matsuda, and M. Tanimoto, *AUE-02-93*; L. L. Chau, H-Y Cheng, W.K. Sze, H. Yao, and B. Tseng, *Phys. Rev. D* **43** (1991) 2176; N. G. Deshpande and J. Trampetic, *Phys. Rev. D* **41** (1990) 895; M. Bauer, B. Stech, and M. Wirbel, *Z. Phys. C* **43** (1987) 103.
5. J.P. Alexander *et al.* (CLEO), *ICHEP94 Ref. GSL0160* (1994).

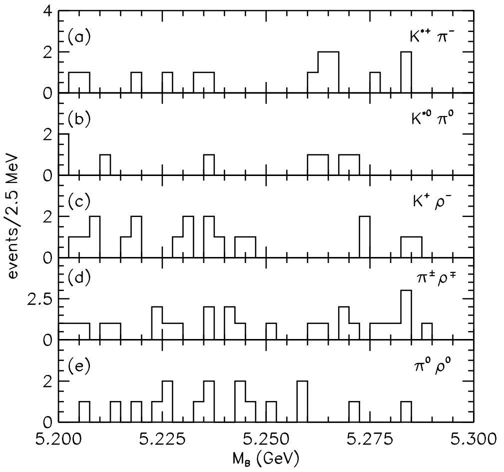

Fig. 2. Beam-constrained mass for (a) $B^0 \to K^{*+}\pi^-$, (b) $B^0 \to K^{*0}\pi^0$, (c) $B^0 \to K^+\rho^-$, (d) $B^0 \to \pi^\pm\rho^\mp$, and (e) $B^0 \to \pi^0\rho^0$ candidates.

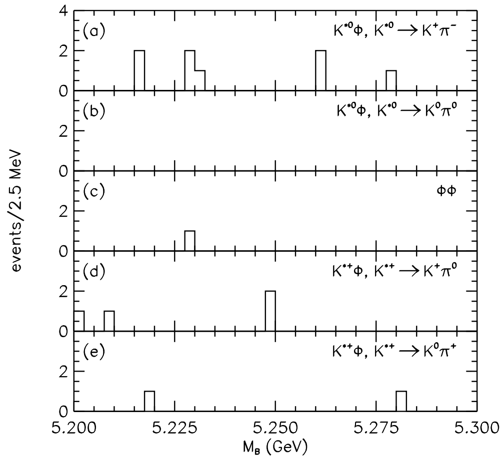

Fig. 3. Beam-constrained mass for $B \to K^*\phi$ and $\phi\phi$ candidates: (a) $K^{*0} \to K^+\pi^-$, (b) $K^{*0} \to K^0\pi^0$, (c) $\phi\phi$, (d) $K^{*+} \to K^+\pi^0$, and (e) $K^{*+} \to K^0\pi^+$.

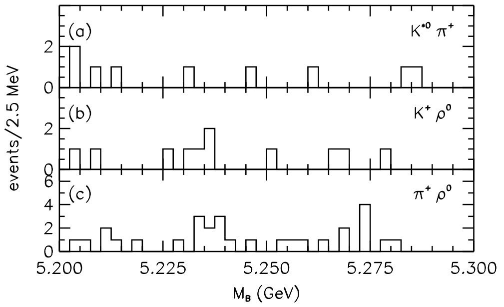

Fig. 4. Beam-constrained mass for (a) $B^+ \to K^{*0}\pi^+$, (b) $B^+ \to K^+\rho^0$, and (c) $B^+ \to \pi^+\rho^0$ candidates.

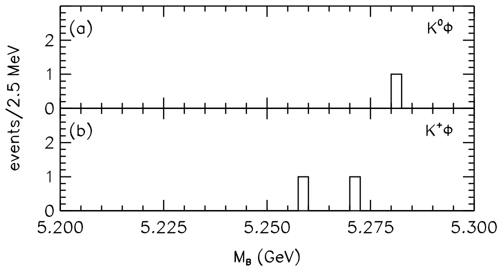

Fig. 5. Beam-constrained mass for (a) $B^0 \to K^0\phi$ and (b) $B^+ \to K^+\phi$ candidates.

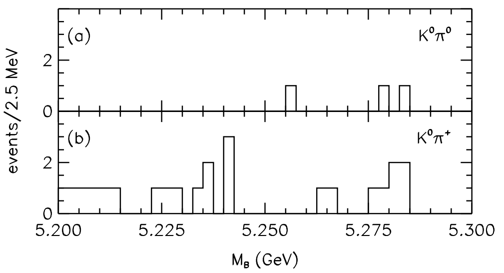

Fig. 6. Beam-constrained mass for (a) $B^0 \to K^0\pi^0$ and (b) $B^+ \to K^0\pi^+$ candidates.

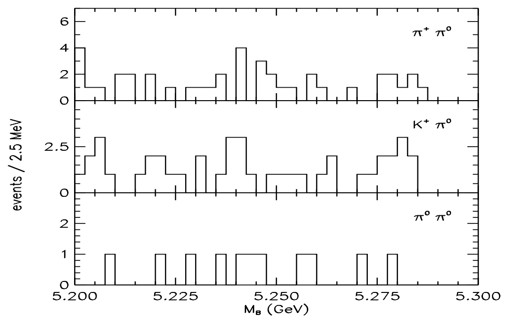

Fig. 7. Beam-constrained mass for (a) $B^+ \to \pi^+\pi^0$, (b) $B^+ \to K^+\pi^0$, and (c) $B^0 \to \pi^0\pi^0$.